Materials Research Express

PAPER

Experimental and Digimat-FE based representative volume element analysis of exceptional graphene flakes/aluminium alloy nanocomposite characteristics

Biswajeet Nayak[1] **and R K Sahu**[2,3]

[1] Department of Mechanical Engineering, S.R.M. Institute of Science and Technology, Kattankulathur-603203, Tamil Nadu, India
[2] Department of Mechanical Engineering, National Institute of Technology Karnataka, Surathkal-575025, Karnataka, India
[3] Author to whom any correspondence should be addressed.

E-mail: ranjeet.nitrkl5@gmail.com

RECEIVED
5 September 2019

REVISED
3 October 2019

ACCEPTED FOR PUBLICATION
7 October 2019

PUBLISHED
18 October 2019

Keywords: graphene flakes, aluminium alloy (AA6005) nanocomposite, microstructure, characterization, Digimat-finite element, RVE model

Abstract

The present article is focused on the in-house synthesis of graphene nano-flakes (size range: 3–8 nm) reinforced Al-alloy (AA6005 series) nanocomposites using stir casting process. The microstructure of the obtained Al nanocomposites at different concentration of flake shaped graphene nanoparticles (GRNPs) show that the particles at 2 wt% and 4 wt% found to be distributed extensively on the surfaces of Al alloy matrix but observed negligible across the grain boundary whereas in the case of 6 wt% concentrated developed composite specimen, the GRNPs were observed to be well dispersed both on the surfaces and grain boundary of the matrix. With the addition of the particles, there found to be the formation of more voids in the nanocomposite specimens. The experimental characterization results reveal that with the increase in graphene content to 6 wt%, the tensile strength, compressive strength, impact energy, hardness and wear resistance of the nanocomposites were increased by 9% to 36%, 30% to 44%, 9.8 J, 36.03 HRB and 33% respectively as compared to unreinforced alloy. It was observed that the composites with increased concentration of reinforcement exhibits brittle behaviour and at 6 wt% GRNPs, the elongation is almost found to be 50% lower than the unreinforced one. Further, a 3D microstructure representative volume element (RVE) model of aluminium nanocomposite is generated using Digimat-FE software. Then, microstructural deformation behaviour of the nanocomposite is realized by RVE model. The simulation results reveal that the tensile property of the aluminium nanocomposites predicted using RVE model is in well agreement with the experimental values.

1. Introduction

In this millennium, nanotechnology has gained considerable importance with its application in the multidisciplinary scientific field for the aim of producing new materials at nano level scale known as nanostructured materials. Nanostructured materials are those materials which are having at least one dimension in a range of 1 to 100 nm. These nanostructured materials include nanoparticles, nanocomposites, nanotubes, nanorods, and nano-thin films, etc However, in recent time nanocomposites in the field of nanotechnology has drawn a lot of attention among the researchers and have become a fast-growing field. Nanocomposites are those materials in which the dispersed phase is in the nanometer range. These materials have played a significant role in scientific, industrial and medical fields because of their extraordinary properties as compared to conventional composites. Their uniqueness arises due to the large surface area to volume ratio of the dispersed phase indicating a large fraction of atoms present on the dispersed phase surface that are chemically unsaturated. Among various nanocomposites, metal matrix nanocomposites (MMNCs) have gained a remarkable research and market attention because of their novel mechanical, physical, thermal, electrical, tribological, permeability,

optical properties, etc and interdisciplinary emerging applications [1]. Currently, aluminium matrix nanocomposites (AMNCs) have attracted significant curiosity among the researchers owing to their reasonable cost, low-weight structure cum extraordinary aforesaid properties and promising applications in automotive components, aircraft and space structures, defence, railway brakes, electronics, thermal management systems, household appliances, recreational and sporting goods, etc [2–10]. Different promising methods like stir casting, spray casting, squeeze casting, cold drawing and powder metallurgy has been established for the preparation of aluminium composites containing micron-size reinforcements [11, 12]. But, among the methods mentioned above, stir casting is widely considered because it is simple, flexible and low-cost method, and causes negligible damage to the reinforcement during composites fabrication.

Rahman *et al* [13] fabricated aluminium matrix composites with different concentration of SiC (0, 5, 10 and 20 wt%) using stir casting technique. The tensile strength and hardness of the reinforced aluminium composites was found to be increased with respect to un-reinforced one and observed to be maximum at 20 wt% SiC. Also, found that there is a maximum reduction in wear of the composites at 20 wt% SiC. Micro-structural examination revealed the non-homogeneity nature of the reinforced composites with the formation of porosities. Sivananth *et al* [14] studied the characterization of TiC reinforced Al metal matrix composite prepared by stir casting process at three different concentration of TiC particulates (10, 12 and 15 wt%) and are in the size of 325 meshes. They have conducted the tensile and impact test and also studied the microstructure of the composites. They found that the tensile strength was increased as compared to the unreinforced Al and observed to be maximum at 15 wt% TiC. The brittle nature of the test samples found to be increased with the increase in wt% of TiC particles in the Al matrix. Yolshina *et al* [15] investigated the synthesis and properties of graphene and graphite based aluminium metallic material. The density and tensile strength of the unreinforced aluminium were found to be 2.7 g cm^{-3} and 41.46 MPa. But, after incorporating 2 wt% of graphene sheets and graphite, tensile strength has found to be increased to 48.1 MPa and 43.92 MPa respectively, while the density decreased to almost 2.4 g cm^{-3} in both the cases. Shankar [16] studied the mechanical characteristics of glass reinforced aluminium matrix composite prepared by stir casting. They used matrix material Al 6061 alloy and reinforced with 3 to 12 wt% glass particulates. They used glass particulates of different sizes- 75, 88, 105 and 250 μm. They found that by addition of reinforcement up to 9 wt% the tensile strength and hardness found to be increased and thereafter decreased. Sharifi *et al* [17] mixed Al powder with B_4C nanoparticles (concentration: 5 wt%, 10 wt%, and 15 wt%) using a ball milling process. Nanocomposite samples were fabricated by hot pressing of milled powders. They found that the samples with 15 wt% have a compressive strength of 485 MPa and hardness of 164 HV whereas pure Al showed the compressive strength of 130 MPa and hardness 33 HV. Devaraju and Pazhanivel [18] carried out hardness, wear and compressive strength characterization on Al 1100 alloy composites reinforced with B_4C particles (average size—30 μm). The composite samples produced by stir casting process at a concentration of 2.5%, 5%, 7.5% and 10% by weight of reinforcement. The hardness property of the samples found to be increased due to the uniform dispersion of B_4C in the aluminium matrix. The wear rate observed to be less when the sample subjected to a load of 16 N at 7.5 wt% of reinforcement. Moreover, maximum compressive strength was found at 7.5% of B_4C. Padmavathi and Ramakrishnan [19] prepared Al 6061 matrix based composites using stir casting by reinforcing combined multi-walled carbon nanotubes (MWCNT) (concentration-0.5 wt% and 1 wt%) and SiC (concentration-15 wt%) in the matrix. They performed wear and hardness test on the composite samples. The hardness of the samples found to be increased with increase in the concentration of MWCNT. Also, over the addition of MWCNT, the coefficient of friction found to be reduced and resulted in low wear rate as compared to pure aluminium. James *et al* [20] synthesized a hybrid composite material by incorporating SiC and TiB_2 particles in Al matrix using stir casting. They studied the wear, tensile and hardness behaviour of the composites and the effect of the reinforcements on the properties of the samples. It was found that the wear resistance of the composite samples significantly enhanced with the addition of TiB_2 particles but when the concentration of TiB2 exceeds 10 wt%, the wear resistance behaviour got reduced. The tensile strength and hardness of the composites considerably increased with the addition of SiC particles. Imran *et al* [21] prepared graphite plus bagasse ash reinforced Al 7075 composite materials using stir casting at a discrete concentration of 1%, 3%, 5% by weight of graphite and 2%, 4%, 6% by weight of bagasse ash. With an increase in the concentration of graphite and maintaining 2 wt% of bagasse ash, there is an improvement in the characteristics like ultimate tensile strength and Brinell hardness number (BHN) of the composite specimens. The similar trend was observed by changing the content of ash while maintaining 1 wt% of graphite. Xavier and Suresh [22] synthesized aluminium matrix composites by reinforcing the different concentration of stone dust particles using stir casting technique. The wear test was performed on the composite specimens using pin on disc (62 HRC) method and compared with the unreinforced specimens. The coefficient of friction found to be reduced by an increase in load and this is caused due to softening of the composite through frictional wear. As a result, the wear resistance of the composite specimens observed to be enhanced with respect to the unreinforced one.

The properties of single phase materials can be determined either experimentally or by numerical simulation. But, the properties of multi-phase materials in a certain range with exceptional microstructures cannot be evaluated experimentally [23]. The idea of the first model was developed to determine the mechanical, electrical and thermal characteristics of simple structured multi-phase materials (either particle reinforced with matrix phase or two soluble phases) [24]. A precise 3D micro-structural representation was required for predicting the naturalistic behaviour of a material [25, 26]. The model representing different shapes of particle was generated and parameters like size of the particle and its distribution, agglomeration and neck formation were included in the model. In the model, different volume of pores and contact area of particles for various shapes of particle was considered [27]. Chawla and Chawla [28] compared the 3D microstructural model of respective spherical and ellipsoidal shaped single particle with multiparticle. They concluded that the 3D microstructure concept found to be more adaptive in realizing the material behaviour through numerical simulation. The properties of the complete microstructure of a material can be suitably described by representative volume element (RVE) model [29]. RVE model represents a small volume of microstructure of a material in which various phases of particular morphology are present and this unit volume behaviour will be similar to its bulk form [30, 31]. The modeling of grain structures reinforced into matrix phase was carried out using mathematical algorithms [32]. A wide variety of diagnostic techniques have been used to characterize the 3D microstructures. These methods include atomic force microscopy, scanning tunnelling microscopy, focused ion beam microscopy, X-ray computer tomography, and ultramicrotomy [26, 33].

RVE modeling technique is a robust tool to simulate the micromechanical behaviour of engineering materials at a low computational cost. Numerous studies have carried out on the simulation of the mechanical behaviour of composite materials, yet RVE modeling of the micromechanical behaviour of metal matrix nanocomposites is not often detailed in the literature. Moreover, the preparation and characterization of aluminium matrix (elemental aluminium/aluminium alloy of different series—Al 1100, 6061 and 7075) composite reinforced with micron size particles were carried out extensively, as it was found from various available literature, whereas, with nanoparticles, it was devoted to a limited extent. The nano-reinforcements like B_4C, MWCNTs, graphite, stone dust particles and few others have been studied. But, the preparation and characterization study of aluminium alloy matrix (AA6005 series) composites reinforced with graphene nanoparticles have yet to be discussed. This could be the alternative for the aforementioned nanoparticles reinforced composites and would be advantageous for potential applications.

Therefore, the present work is focused on the development and characterization of aluminium alloy matrix (AA6005 series) graphene reinforced nanocomposites using stir casting process. Stir casting route is preferred in this study because this method could provide good dispersion of nano-reinforcement within the matrix, better matrix-particle bonding, breaks preform nanoparticle clusters, control matrix structure easily and remove impurities from the surface of the particles. A 3D microstructure RVE model of aluminium nanocomposite was generated using Digimat-FE software. Digimat evaluates the microstructural deformation behaviour of the model. The tensile property of the aluminium nanocomposites was determined using numerical simulation and the simulation results are compared with the experimental values.

2. Experimental work

In the present work, the matrix material was taken as aluminium alloy (AA6005) purchased from Junaid Steel & Alloys, Chennai and reinforcement as graphene nanoparticles (in the form of flakes) from Adnanotech Pvt. Ltd, Shimoga, India. Al alloy (AA6005) was chosen because of its low weight, high strength, good corrosion resistance, good casting properties, etc after casting [14, 34, 35] and GRPNs exhibit extraordinary properties like high stiffness, thermal conductivity, impermeable to gases, high mobility of charge carriers and optically transparent. The microscopic image of AA6005 sample and preform GRPNs (in the form of flakes) is shown in figure 1.

The Al alloy sample comprises of 97.25 wt% Aluminium with 2.75 wt% other elements (Mg—1.08 wt%; Fe—0.17 wt%; Si—0.63 wt%; Zn—0.32 wt%; Mn—0.52 wt%; V—0.01 wt%; Ti—0.02 wt%). The physical and mechanical properties of the preform graphene nanoparticles (GRNPs) are listed in table 1.

The detail description of the preparation of GRNPs reinforced Al MMCs using stir casting process is as follows. The bulk Al alloy was weighed and cut into small pieces and placed in the crucible (size number- 6 and total capacity—2 kg) along with degasser and coverall powder. Degasser and coverall powder were used to remove the impurity from the molten metal and retain the temperature in the crucible, respectively. The Al alloy was melted in the electric furnace at 850 °C and at the same time, GRNPs loaded in another crucible also placed in the furnace for 2 hours to avoid moisture content, if any, as shown in figure 2(a). The preheated GRNPs were mixed with molten Al alloy by mechanical stirrer at a speed of 250 rpm as shown in figure 2(b). The mixture was poured into the preheated die and allowed for solidification for a few hours, and finally, the solidified material as

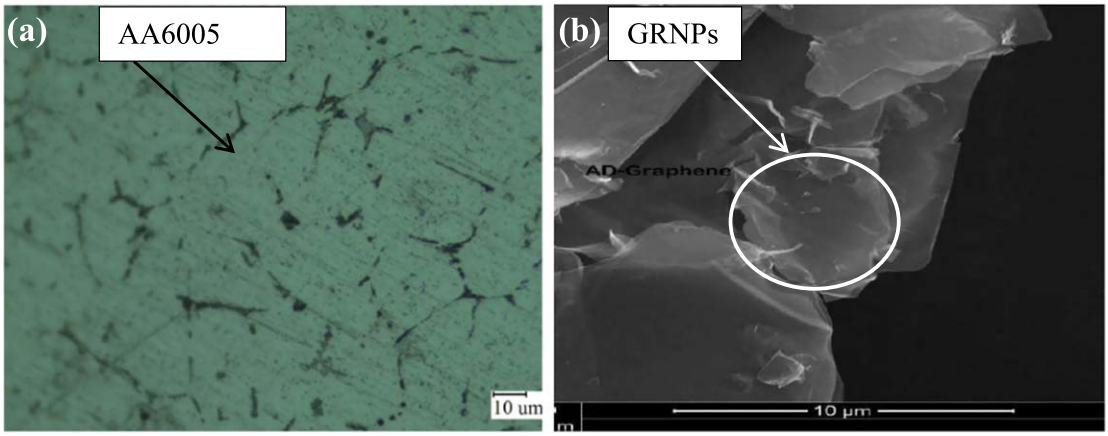

Figure 1. (a) Optic image of AA6005 alloy sample, (b) SEM image of preform GRNPs.

Table 1. Properties of preform GRNPs.

Sl. No.	Physical properties	Description	Mechanical properties	Values
1	Colour	Black powder	Tensile strength	130 GPa
2	Purity	>99%	Elastic modulus	1 TPa
3	Average thickness (Z)	3–8 nm	Thermal conductivity	5000 W/m K
4	Average lateral dimension (X&Y)	5–10 μm	Electrical conductivity	10×10^7 S m^{-1}
5	Number of layers	2–4 layers		
6	Surface area	250 m^2 g^{-1}		

Al nanocomposite specimens is taken out from the die as shown in figure 2(c) and (d). In this study, aluminium matrix nanocomposite test specimens with three different concentrations (2 wt%, 4 wt% and 6 wt%) of GRNPs were cast for mechanical characterization. The unreinforced Al alloy specimens are also prepared for comparison.

The properties like tensile, compression, impact, hardness and wear of the prepared aluminium nanocomposites are characterized using various diagnostic equipments. The tensile and compression test specimens (figures 3(a) and (b)) were prepared according to the ASTM-E08 [36] and ASTM E09 [37], respectively from the cast specimens. The tests were conducted on the specimens using a 100 kN servohydraulic Instron universal Testing Machine at room temperature. The impact test specimens (figure 3(c)) were prepared from the cast specimens as per ASTM-E23 [38] and tests were carried out using the Charpy impact test machine. The hardness tests for the specimens were carried out as per ASTM-E18 standard in an FIE RASNE-3 Rockwell hardness testing unit. A ball indenter was pressed on the specimens at a load of 100 kg and five readings were taken for each sample to ascertain precision hardness value. The Rockwell test method is chosen for hardness testing because it is a quick and cost-effective process, the hardness value is directly readable irrespective of surface quality of the specimen and optical evaluation is not required.

Further, using pin-on-disc setup (Make: DUCOM; Model: Wear & Friction Monitor TR-201), the wear tests were conducted for the specimens (figure 3(d)) as per ASTM G99 under dry conditions. The aluminium nanocomposite test specimens as shown in (figure 3(d)) were used as pin specimens (length: 30 mm and diameter: 10 mm) and the pinned specimen was positioned perpendicular to the counter face of a disc (EN31 steel) having diameter 60 mm. In the present work, the disc rotates at 500 rpm and the pinned specimen was loaded against the disc by means of dead weight loading systems. The wear test was carried out for three samples each for unreinforced Al alloy and different concentrated specimens (2 wt%, 4 wt% and 6 wt%) under the normal loads of 5 N, 10 N, 15 N and duration of 5 min for each sample, and subsequently wear loss was recorded by weighing the specimen. During wear test, the parameters such as relative speed, duration of experimental run and load applied are kept constant throughout for all the experiments.

3. Experimental results

The microstructural and mechanical characterization results of the developed graphene nanoparticle reinforced Al MMCs are discussed in this section.

Figure 2. (a) Al alloy melting and GRNPs heating inside the furnace; (b) mixing of preheated GRNPs with melt by mechanical stirrer; (c) pouring of mixture in the preheated die; (d) prepared Al nanocomposite specimens.

3.1. Microstructural characterization

The microstructure of the Al nanocomposite specimens cast with different concentrations was examined by using a scanning electron microscope-SEM (FEI Quanta FEG 200) to study the distribution of GRPNs in the Al alloy matrix. (figures 4(a)–(c)) shows the SEM images of a polished cross-section of Al alloy- 2 wt%, 4 wt% and 6 wt% GRNPs reinforced composite specimens respectively. It is evident from the (figures 4(a), (b)) that the GRNPs represented by bright spots are distributed extensively on the surfaces of the Al alloy matrix but found to be negligible across the grain boundary. However, in the case of 6 wt% concentrated developed composite specimen (figure 4(c)), the flake-shaped GRNPs were observed to be well dispersed on the surfaces and at the grain boundary of the matrix. This was attributed due to the good wetting mechanism resulted from matching between the FCC crystal structure of Al and nature of GRNPs. The presence of graphene particles at the matrix grain boundary ensures a strong interfacial bond between them due to the pinning of particles on the grain-boundary structure. This will result in the strong opposition to the deformation across grain boundaries during loading and thus increase in ultimate strength of the composites. Moreover, at some locations, voids/porosities are formed at 6 wt% GRNPs (figure 4(d)). This is due to the entrapment of air between the particles during molten alloy infiltration and variation in solidification rate within the material. So, with further increase in the concentration of GRNPs there found to be increased in the formation of voids.

Figure 5 shows the EDAX pattern of the GRNPs/Al alloy developed composite. The analysis was carried out over a one square inch area of figure 4(c) and the pattern shows the characteristic peaks of carbon and aluminium alloyed with other elements like Mg, Si, and Zn. This indicates the presence of graphene particles in the Al alloy matrix. Moreover, it is demonstrated that oxides of aluminium are observed and other negligible impurities were also noticed in EDAX that cannot be excluded.

3.2. Effect of GRNPS on mechanical properties

The tensile and compression properties of unreinforced cast Al alloy and GRNPs/Al alloy composites are provided in table 2.

From the tensile test results, it was observed that with the addition of GRNPs in Al alloy melt there is an enhancement of strength of the composites as compared to the unreinforced Al alloy. This is because the

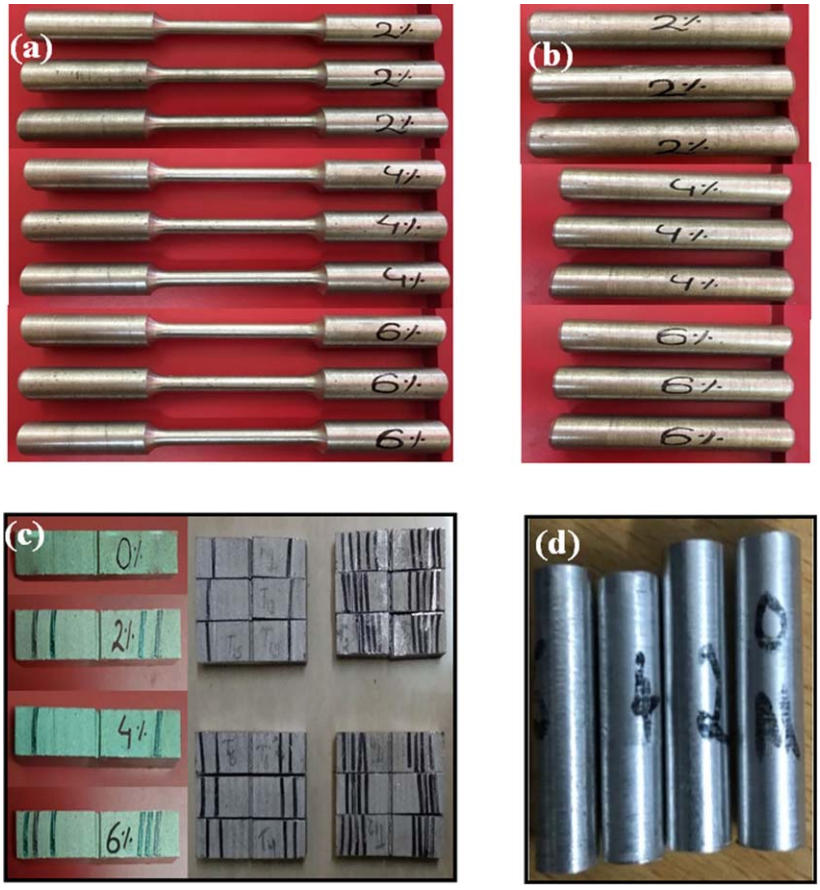

Figure 3. (a) Tensile specimens; (b) compression specimens; (c) impact specimens; (d) wear test specimens.

graphene content in the aluminum alloy matrix strongly influences the enhancement of the mechanical properties of the GRNPs/ aluminum alloy composites. The ultimate tensile strength and yield strength of Al-6 wt% GRNPs increase up to 135.53 MPa and 118.59 MPa respectively. The increase in strength is due to the strong interfacial bonding between the reinforcement and the matrix and grain strengthening effect. Also owing to the fine eutectic mixing of silicon in the matrix and forming globules along with graphene particles, the strength is increased. Moreover, with the increase in the concentration of GRNPs the resistance to plastic deformation increases, thereby increasing ultimate tensile strength. It is found that the % elongation decreased due to the addition of particles indicating the brittle behaviour (reduced ductility) of composites (figure 6(a)). The improvement in strength accompanied by reduction of elongation is observed to be significant as compared to the literature [39, 40]. The aluminium composite specimens reinforced with 6 wt% GRNPs shows elongation of almost 50% lower than that of unreinforced one and this is due to the above-mentioned statement. The tensile test specimens after failure are shown in figure 6(b).

It was observed from the table 2 that with the increase in the concentration of reinforcements (2, 4 and 6 wt%), the compressive strength of Al alloy matrix based nanocomposite test specimens found to be increased monotonously by 30.51%, 33.89%, and 44.21% respectively as compared to the unreinforced cast specimen. This is due to the presence of dense graphene particles at higher concentrations across the matrix grain boundary that impedes the dislocation movement. Visual identification of the deformed specimens after the compression test as shown in (figures 6(c)–(f)) also confirms that Al-6 wt% GRNPs specimen displayed increased compressive strength. The impact energy of the developed test composite specimens reinforced with GRNPs at different concentrations is shown in (figure 7(a)). It is inferred from the figure that increasing wt% of GRNPs in Al alloy matrix, the composites withstand more impact load. This is because of the strong semi-metallic characteristic of graphene which improves the bonding between reinforcement and matrix. But, in case of unreinforced Al alloy, due to the absence of graphene particles, the crack could initiates from the Al alloy matrix area and quickly propagates in various directions without any obstruction and thus the impact energy is reduced. The impact energy of Al-6 wt% GRNPs specimens found to be high (i.e. absorbs more energy during impact testing) and this could be due to the presence of highly dense GRNPs in the matrix. The impact test specimens after fracture are shown in figure 7(b).

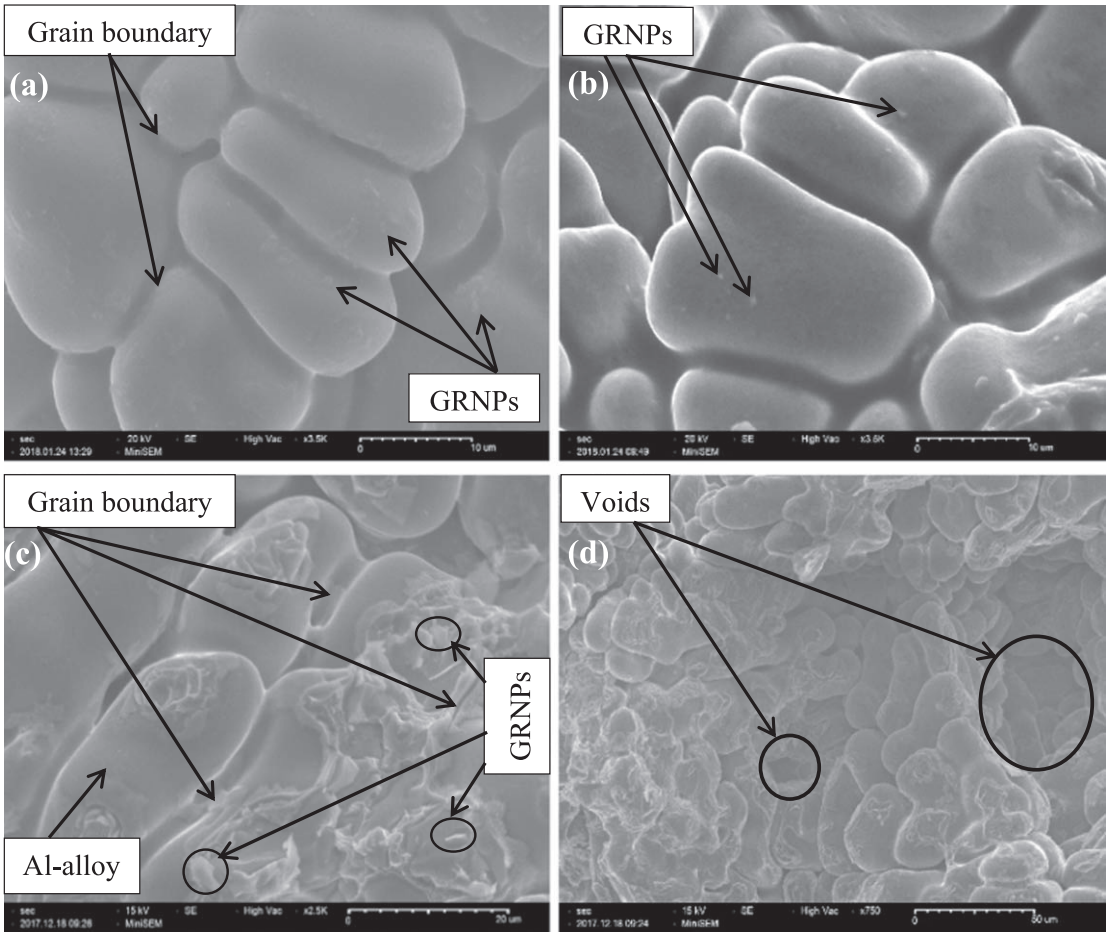

Figure 4. SEM images of GRNPs/Al alloy composite specimens—(a) 2 wt%; (b) 4 wt%; (c) 6 wt%; (d) formation of voids at 6 wt% concentration.

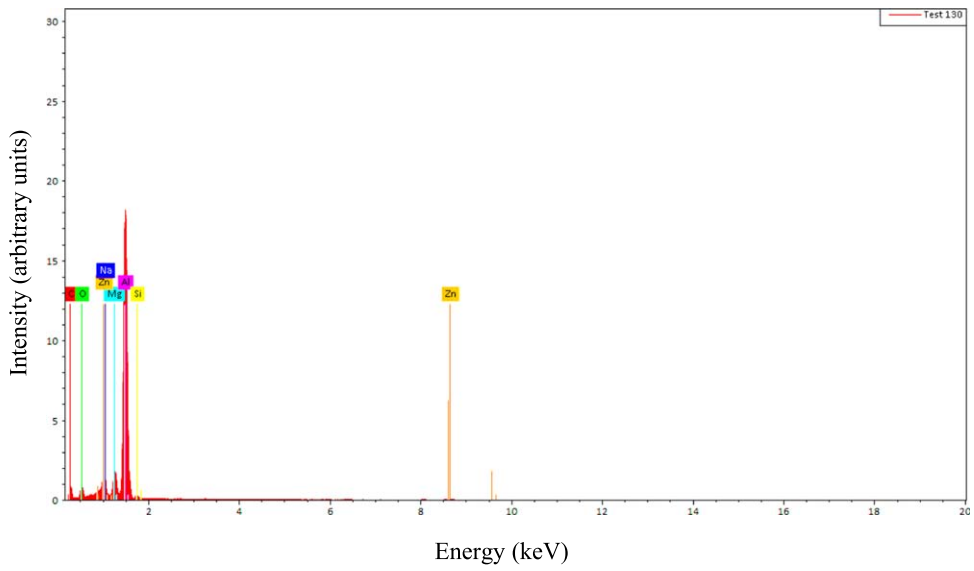

Figure 5. EDAX pattern of the GRNPs (6 wt%)/Al alloy developed composite.

The Rockwell hardness of unreinforced Al alloy as shown in table 2 is found to be 25.87 HRB and with increasing GRNPs content, the hardness of Al alloy nanocomposite specimen reinforced with 6 wt% GRNPs is found to be 61.9 HRB. It was observed from the table that the hardness of the developed GRNPs/Al alloy composite specimens is directly proportional to the concentration of GRNPs up to 6 wt%. The hardness of

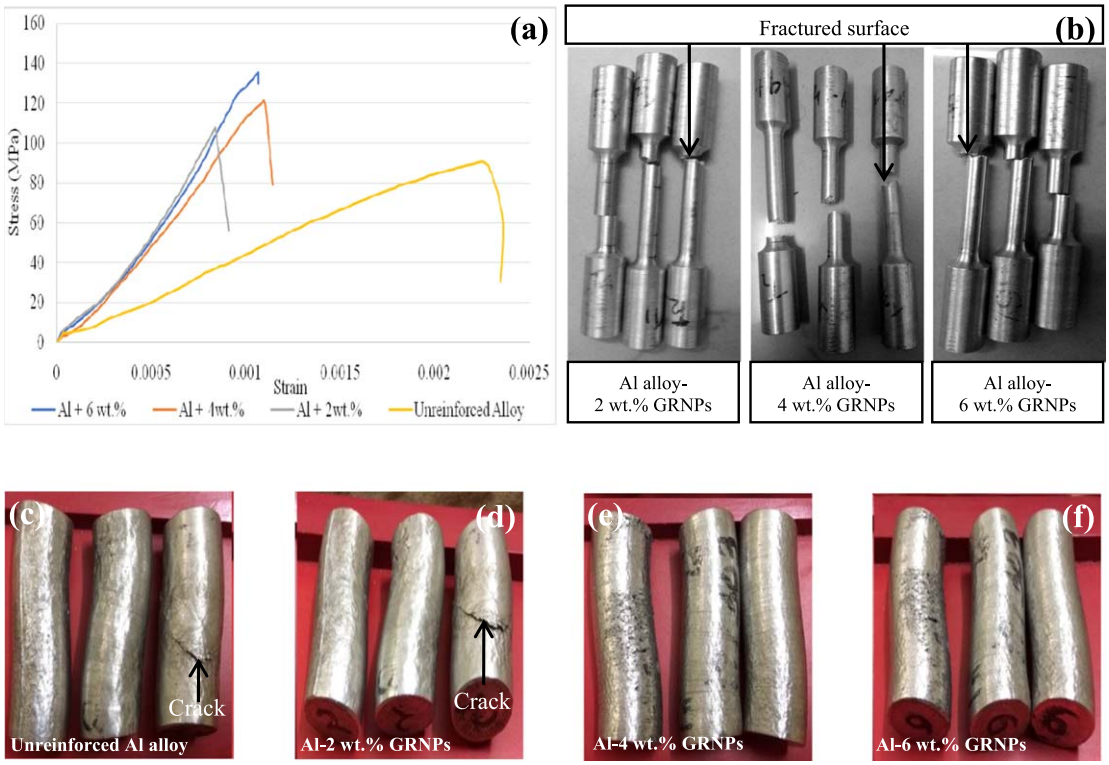

Figure 6. (a) Tensile stress-strain behaviour of GRNPs/Al alloy nanocomposites at different concentrations; (b) tensile test specimens after failure; (c)–(f) compressive strength comparison of deformed nanocomposite specimens at different concentrations (figure (d) and (f)) [41]).

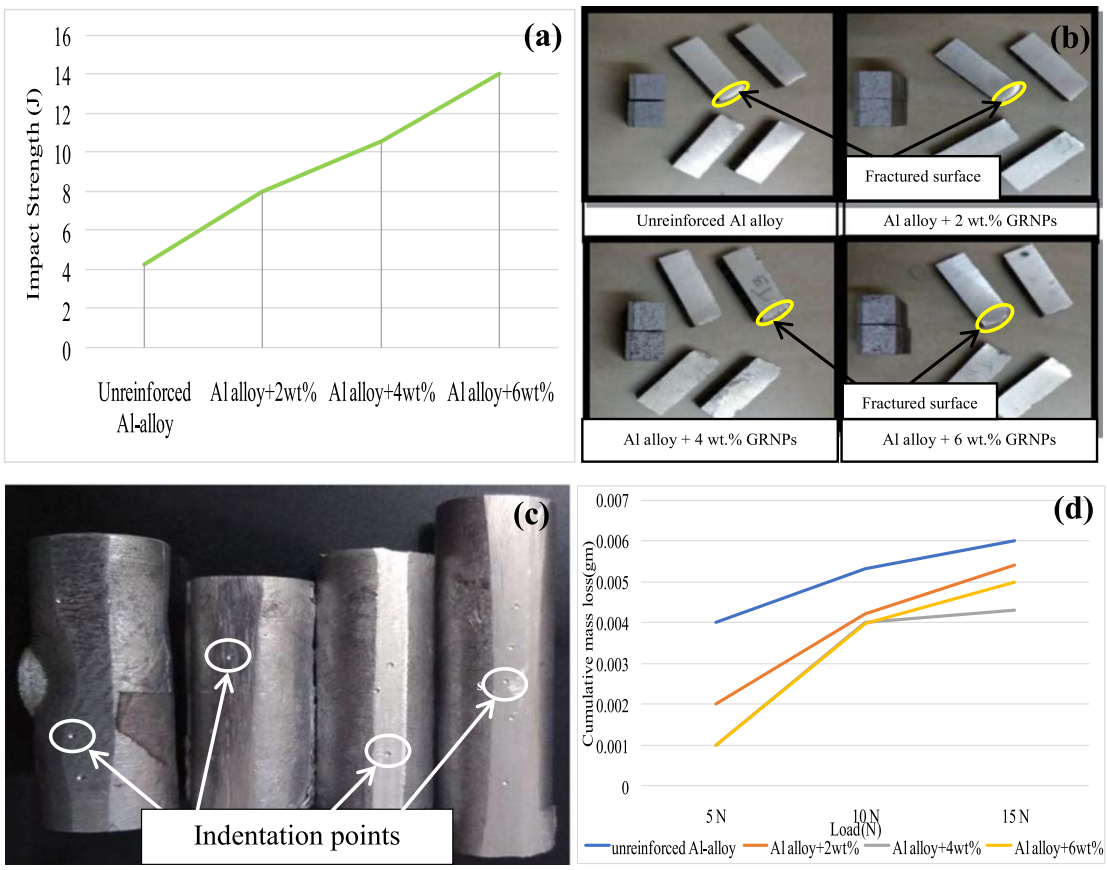

Figure 7. (a) Impact energy comparison of the different test composite specimens; (b) impact test specimens after fracture; (c) Rockwell hardness tested samples; (d) variation of cumulative mass loss in different test composite samples under applied loads.

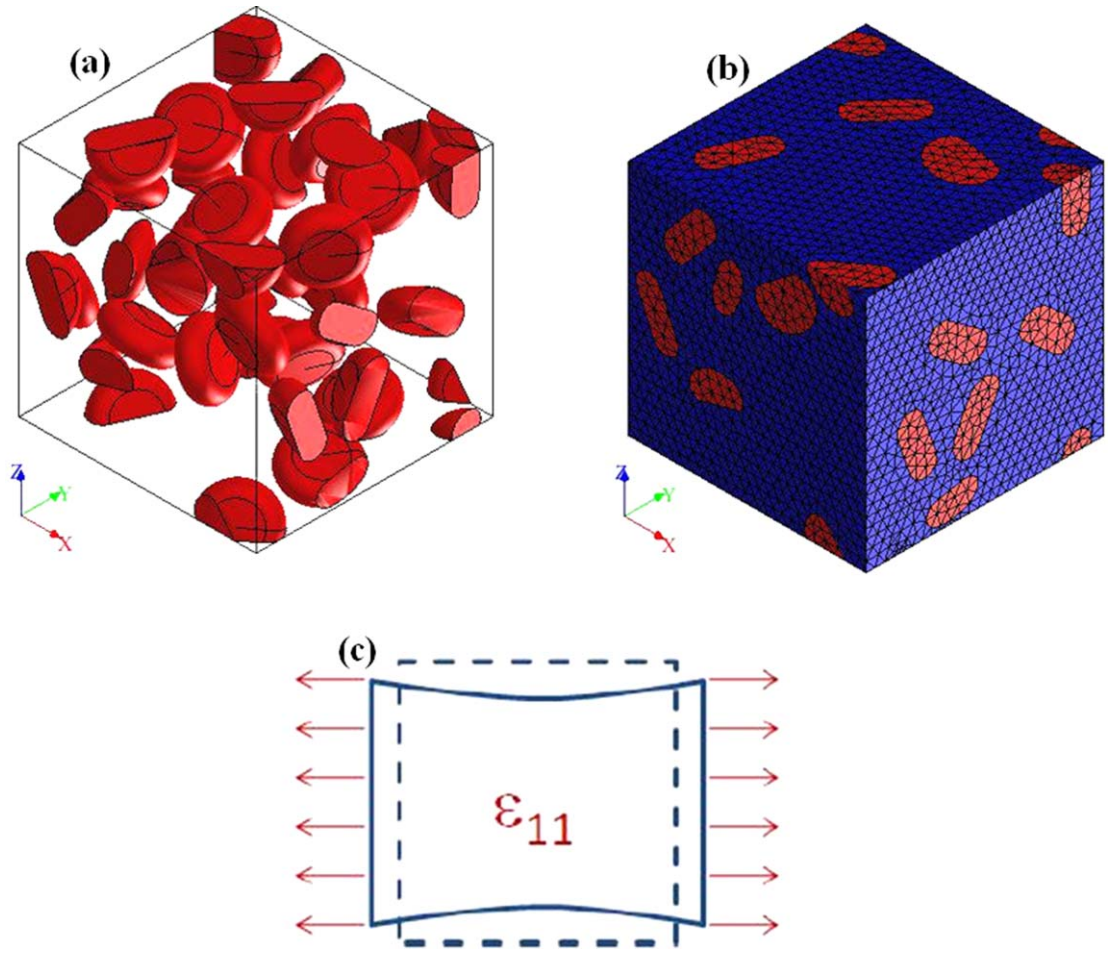

Figure 8. (a) Generated 3D RVE model; (b) meshing of RVE model; (c) RVE under uniaxial tensile loading.

Table 2. Properties of test specimens.

Sl. No.	Test specimens	Ultimate tensile strength (MPa)	Yield strength (MPa)	Compressive strength (MPa)	Rockwell hardness (HRB)
1	Unreinforced cast Al alloy	98.14	81.8	325.18	25.87
2	Al alloy-2 wt% GRNPs	107.87	91.54	424.40	33.5
3	Al alloy-4 wt% GRNPs	121	98	445.63	45.72
4	Al alloy-6 wt% GRNPs	135.53	118.59	468.96	61.9

nanocomposite specimens is at least 1.25 to 2.5 times higher than that of unreinforced alloy. The improvement in hardness of the composite specimens is due to the presence of a large number of stiff and strong graphene flakes (exhibit significant surface area to volume ratio) in the Al alloy matrix (mostly on the grain boundaries and part of them inside the grain of Al alloy matrix) that could effectively impede the movement of dislocations. Also, may be attributed to the strong interaction between the GRNPs and Al alloy matrix at the interface which can transfer the load efficiently from the matrix to the reinforcement. Figure 7(c) shows the Rockwell hardness tested samples of different concentrations of graphene. As shown in figure 7(d), the wear is found to be more in unreinforced Al alloy samples as compared to the GRNPs/Al alloy nanocomposite samples and observed to be maximum at the load of 15 N. But, with the increased addition of GRNPs, the wear in Al nanocomposite samples gets reduced. It is attributed to the hard GRNPs which is exposed in between two surfaces sliding against each other acts as a dry lubricant and prevents the Al alloy matrix from further wear if the concentration is increased to 6 wt%.

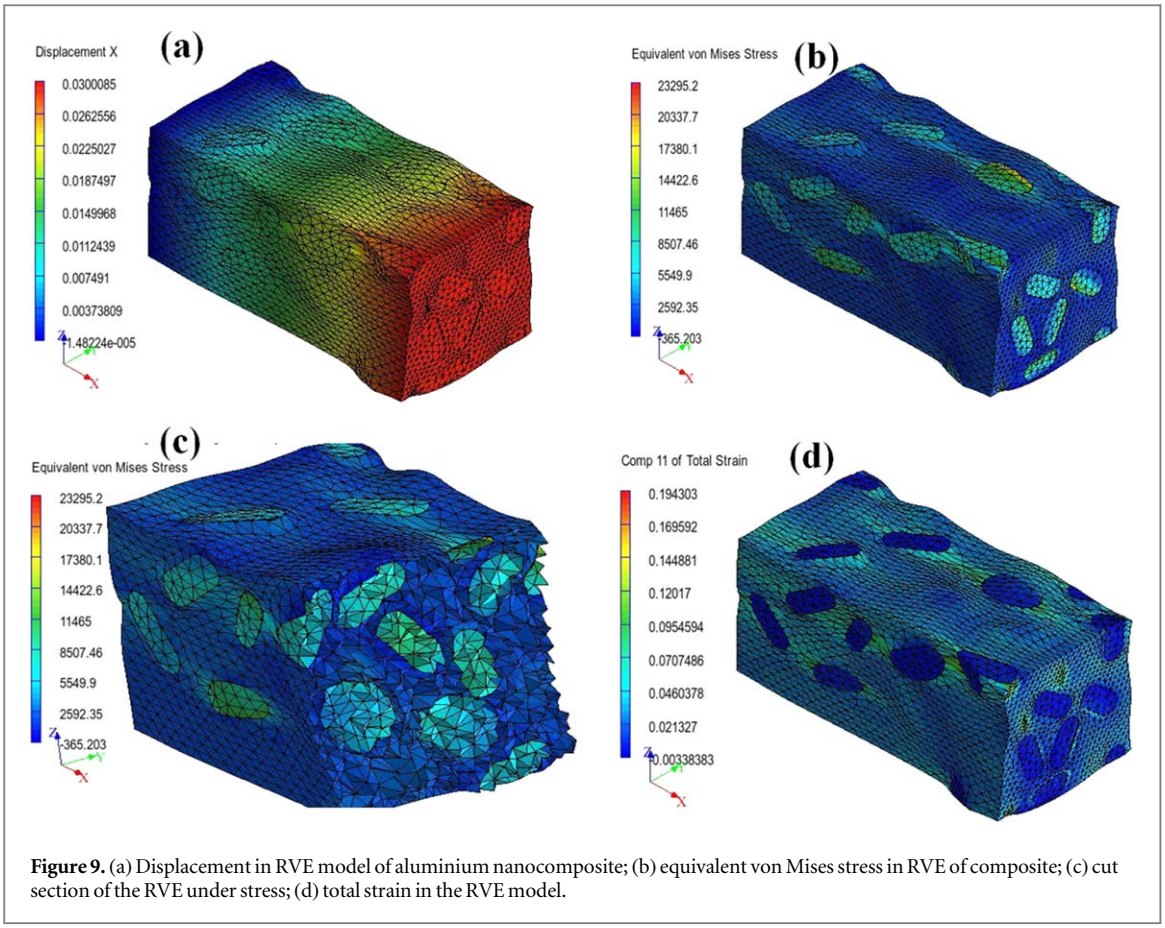

Figure 9. (a) Displacement in RVE model of aluminium nanocomposite; (b) equivalent von Mises stress in RVE of composite; (c) cut section of the RVE under stress; (d) total strain in the RVE model.

4. Micro scale numerical simulation

4.1. Description of creation of RVE model

In the present article a RVE technique with incorporated particulate inclusions is developed to predict the tensile behaviour of aluminium nanocomposites. The Digimat-FE software is used to create 3D microstructure RVE model of aluminium nanocomposite. The RVE microstructure model is comprised of aluminium matrix and graphene particulate (as flake like shape) inclusions with assumed perfectly bonded interface. Through proper tuning of parameters, the size and dispersion of particulate inclusions in a nanocomposite material can be precisely stated. The size of the RVE is considered as very small so that computational time will be less and homogenous stress-strain relation can be expected in the entire RVE. The input parameters in Digimat-FE are taken as follows: aluminium—elastic constant 70 GPa, density 2.70 g cm^{-3} and Poisson's ratio 0.33, and GRNPs —elastic constant 1020 GPa, density 2.1 g cm^{-3} and Poisson's ratio 0.28. The RVE model was generated (figure 8(a)) by assigning the volume fraction, shape, distribution of inclusion phase and the minimum relative distance between inclusions. RVE mesh was generated by Digimat-FE with tetra element size 0.04 (figure 8(b)).

The application of boundary condition to the RVE model is the most important step during computational process. In this paper, under static state of balance mix boundary condition (MBC) was applied to the 3D RVE model using a set of equations and reference points [42]. In MBC, in one part the displacements will be applied to the RVE and in other part the tractions will be applied. The degree of freedom (DOF) of the nodes on the outside faces is related by the DOF of the reference point using equations with constraints. The MBCs and stress applied in the x-direction to the 2D RVE (figure 8(c)) was permitted to show the macroscopic equivalent von Mises stress state of the nanocomposites under uniaxial tensile loading.

4.2. Simulation results

The simulation results along with discussion on the validation of RVE model is shown clearly in this section. In this paper RVE model was generated using Digimat-FE, and by assigning all the pre-processing conditions RVE model was exported to Digimat Solver. The displacement in the RVE model of aluminium nanocomposite (Al + 6 wt% graphene particulate inclusions) under uniaxial load condition is shown in figure 9(a).

The equivalent von Mises stress in the RVE model (figure 9(b)) demonstrates that both the phases (aluminium and graphene particulates) are perfectly bonded with each other because of the high strength of

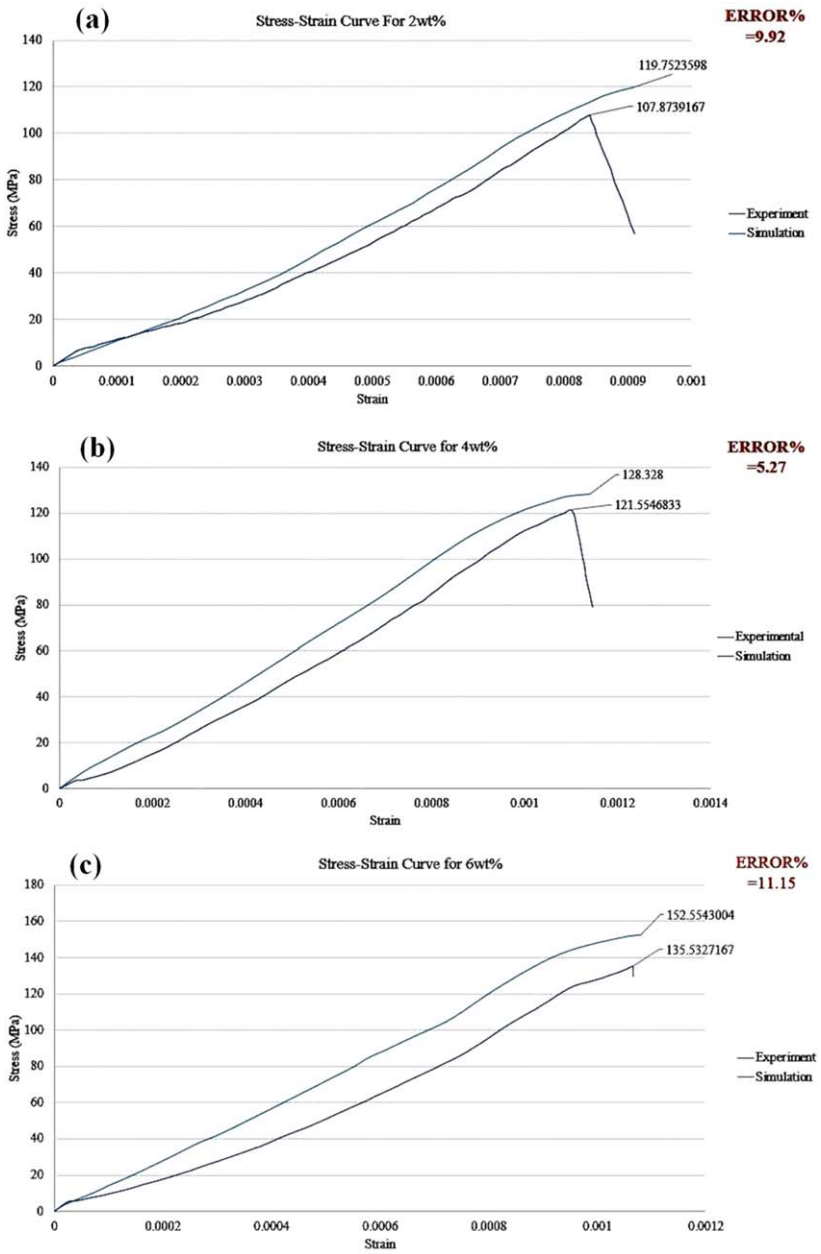

Figure 10. Comparison between simulation and experimental results: stress-strain relation plots for (a) Al + 2 wt% GRNPs; (b) Al + 4 wt% GRNPs; (c) Al + 6 wt% GRNPs.

GRNPs as compared to the Al matrix. The load applied to the RVE model is primarily transferred to the matrix phase and then distributed to the inclusion phase. As a result, maximum stress is induced in the inclusion phase which is ascertained in figure 9(c). The investigation on the state of stress will be useful to point out the defects occurred. The main reasons of failure of nanocomposites during the stage of both manufacturing and their applications could be due to the originated defects and its escalation under applied stress. This can be realized from the figure 8(c) where deformation of RVE model of nanocomposite takes place. The total strain in the RVE model in x-direction (figure 9(d)) clearly shows that strain in the inclusion phase is very small as compared to the matrix phase. This is due to the high elastic modulus characteristics of dispersed GRNPs as compared to the Al matrix phase. Similarly, the RVE model was generated for other concentrations of graphene particulate inclusions in this study, and the stress-strain graphs for different concentrations obtained from Digimat-FE solver in the RVE are presented in figure 10.

The difference between the plots of stress-strain in the RVE of aluminium nanocomposites is a result of the different concentration of the particulate inclusions. The graphs obtained from the simulation are compared with the tensile stress-strain plots obtained from the experimentation for 2, 4 and 6 wt% graphene reinforced

nanocomposites as shown in the figure 10. The results reveal that the tensile properties of the aluminium nanocomposites predicted using RVE model are in well agreement with the experimental values. It can be inferred that the effect of interactions between graphene particulate inclusions and aluminium matrix in the developed 3D microstructure RVE model of aluminium nanocomposites considered being practical. This results in precise Digimat-FE prediction of the stress-strain relation within the nanocomposites. Further, the Digimat-FE simulation can be applicable to detect the damage of nanocomposite microstructure during the loading process in a cost-effective and non-destructive manner.

5. Conclusions

In this article, an experimental approach has been made to develop graphene nanoparticles (GRNPs) reinforced Al-alloy nanocomposites using stir casting process. The nanocomposite materials were synthesized with well-dispersed graphene inclusions inside an aluminium alloy matrix. The reinforcements are in the form of flakes having size—thickness in the range of 3–8 nm and lateral dimension of 5–10 μm, and the concentration was taken as 2 wt%, 4 wt% and 6 wt%. Characterization of the developed nanocomposites was carried out using various diagnostic equipments. Further, 3D RVE model of aluminium nanocomposite was generated using Digimat-FE software and the deformation behaviour under uniaxial tensile load was analyzed. The following conclusions are drawn from the experimental and simulation results.

1. The microstructural analyses showed that at 6 wt% concentrated developed nanocomposite specimen, the GRNPs was found to be well distributed both on the surfaces and at the grain boundary of the Al alloy matrix. But, at lower concentrations (<6 wt%) the dispersion of GRNPs observed to be negligible across the grain boundary.
2. A large amount of porosity was observed in the Al nanocomposites with the increase in the concentration of nano-reinforcements.
3. With the increase in graphene content to 6 wt%, the tensile strength, compressive strength, impact energy, hardness and wear resistance of the nanocomposites were increased by 9% to 36%, 30% to 44%, 9.8 J, 36.03 HRB and 33% respectively as compared to unreinforced alloy.
4. At 6 wt% GRNPs, the elongation was almost found to be 50% reduced than the unreinforced one indicating the brittle behaviour of GRNPs/Al-alloy composites when concentration of reinforcement was increased.
5. The simulation results reveal that the tensile properties of the aluminium nanocomposites predicted using RVE model are in well agreement with experimental values.
6. RVE model created using Digimat-FE permits reproducing the actual deformation of the aluminium matrix with graphene particulate inclusions and precise prediction of the stress-strain relation within the nanocomposites.

Acknowledgments

The authors would like to thank to the Strength of Materials laboratory, Design section, Department of Mechanical Engineering, SRM Institute of Science and Technology, Kattankulathur, India and Omega laboratory, Kattankulathur, India for providing the testing facilities for characterization.

ORCID iDs

R K Sahu https://orcid.org/0000-0001-7999-7955

References

[1] Ajayan P M, Schadler L S and Braun P V 2003 *Nanocomposite Science and Technology* (Germany: Wiley-VCH, Verlag)
[2] Shao P, Yang W, Zhang Q, Meng Q, Tan X, Xiu Z, Qiao J, Yu Z and Wu G 2018 Microstructure and tensile properties of 5083 Al matrix composites reinforced with graphene oxide and graphene nanoplates prepared by pressure infiltration method *Compos. Part A: Appl. Sci. Manuf.* **109** 151–62
[3] Lopez V H, Scoles A and Kennedy A R 2003 The thermal stability of TiC particles in an Al7wt.%Si alloy *Mater. Sci. Eng.* A **356** 316–25
[4] Gopalakrishnan S and Murugan N 2011 Prediction of tensile strength of friction stir welded aluminium matrix TiCp particulate reinforced composite *Mater. Des.* **32** 462–7

[5] Swamy A R K, Ramesh A, Kumar G V and Prakash J N 2011 Effect of particulate reinforcements on the mechanical properties of Al6061-WC and Al6061-Gr MMCs *J. Miner. Mater. Char. Eng.* **10** 1141–52
[6] Poovazhagan L, Kalaichelvan K, Rajadurai A and Senthilvelan V 2013 Characterization of hybrid silicon carbide and boron carbide nanoparticles-reinforced aluminum alloy composites *Procedia Eng.* **64** 681–9
[7] Vencl A, Rac A and Bobic I 2004 Tribological behaviour of Al-based MMCs and their application in automotive industry *Tribology Industry* **26** 31–8
[8] Seyed N P and Asgharzadeh H 2019 Aluminum matrix composites reinforced with graphene: a review on production, microstructure, and properties *J. Critic. Review. Solid State. Mater Sci.* (https://doi.org/10.1080/10408436.2019.1632792)
[9] Khan M, Din R U, Wadood A, Syed W H, Akthar S and Aune R E 2019 Effect of graphene nanoplatelets on the physical and mechanical properties of Al6061 in fabricated and T6 thermal conditions *J. Alloys Comp.* **790** 1076–91
[10] Venkatesan S and Xavior M A 2019 Wear characteristics studies on graphene reinforced AA7050 based composite *Mater. Res. Express* **6** 056501-15
[11] Hashim J, Looney L and Hashmi M S J 1999 Metal matrix composites: production by the stir casting method *J. Mater. Process. Tech.* **92** 1–7
[12] Li J, Zhang X and Geng L 2018 Improving graphene distribution and mechanical properties of GNP/Al composites by cold drawing *Mater. Des.* **144** 159–68
[13] Rahman M H, Rashed A and Mamun H 2014 Characterization of silicon carbide reinforced aluminium matrix composites *Procedia Eng.* **90** 103–9
[14] Sivananth V, Vijayarangan S and Rajamanickam N 2014 Evaluation of fatigue and impact behaviour of titanium carbide reinforced metal matrix composites *Mater. Sci. Eng.* A **597** 304–13
[15] Yolshina L A, Muradymov R V, Korsun I V, Yakovlev G A and Smirnov S V 2016 Novel aluminium-graphene and aluminium-graphite metallic composite materials: synthesis and properties *J. Alloy. Compd.* **663** 449–59
[16] Madhu K Y C and Shankar U 2012 Evaluation of mechanical properties of aluminium alloy 6061- glass particulates reinforced metal matrix composites *Int. J. Mod. Eng. Res.* **2** 3207–9
[17] Sharifi E M, Karimzadeh F and Enayati M H 2011 Fabrication and evaluation of mechanical and tribological properties of boron carbide reinforced aluminium matrix nanocomposites *Mater. Des.* **32** 3263–71
[18] Devaraju A and Pazhanivel K 2016 Evaluation of microstructure, mechanical and wear properties of aluminium reinforced with boron carbide nano composite *J. Sci. Technol.* **9** 1–6
[19] Padmavathi K R and Ramakrishnan R 2014 Tribological behaviour of aluminium hybrid metal matrix composite *Procedia Eng.* **97** 660–7
[20] James S J, Venkatesan K, Kuppan P and Ramanujam R 2014 Hybrid aluminium metal matrix composite reinforced with SiCand TiB_2 *Procedia Eng.* **97** 1018–26
[21] Imran M, Khan A R A, Megeri S and Sadik S 2016 Study of hardness and tensile strength of aluminium-7075 percentage varying reinforced with graphite and bagasse-ash composites *Res. Efficient. Technol.* **2** 81–8
[22] Xavier L F and Suresh P 2016 Wear behaviour of aluminium metal matrix composite prepared from industrial waste *Sci. World J.* **2016** 1–8
[23] Winkler D E R, Staab T E M, Muller T M and Raether F G 2016 Using of novel microstructure generator to calculate microscopic properties of multi-phase non-oxide ceramics in comparison to experiments *Ceram. Int.* **42** 325–33
[24] Ondracek G 1978 On the relationship between the properties and the microstructure of multiphase materials *Mater. Sci. Eng. Technol.* **9** 31–6 https://onlinelibrary.wiley.com/doi/abs/10.1002/mawe.19780090307
[25] Roters F, Eisenlohr P, Hantcherli L, Tjahjanto D D, Bieler T R and Raabe D 2010 Overview of constitutive laws, kinematics, homogenization and multiscale methods in crystal plasticity finite-element modeling: theory, experiments, applications *Acta. Mater.* **58** 1152–211
[26] Mingard K P, Jones H G and Gee M G 2014 Metrological challenges for reconstruction of 3-d microstructures by focused ion beam tomography methods *J. Microsc.* **253** 93–108
[27] Raether F and Iuga M 2006 Effect of particle shape and arrangement on thermoelastic properties of porous ceramics *J. Eur. Ceram. Soc.* **26** 2653–67
[28] Chawla N and Chawla K K 2006 Microstructure-based modeling of the deformation behavior of particle reinforced metal matrix composites *J. Mater. Sci.* **41** 913–25
[29] Schmidt K and Becker J 2012 Generating validated 3D models of microporous ceramics *Adv. Eng. Mater.* **15** 40–5
[30] Ogierman W and Kokot G 2014 Particle shape influence on elastic-plastic behavior of particle-reinforced composites *Arch. Mater. Sci. Eng.* **67** 70–6
[31] Amirmaleki M, Samei J, Green D E, Riemsdijk I V and Stewart L 2016 3D micromechanical modeling of dual phase steels using the representative volume element method *Mech. Mater.* **101** 27–39
[32] Wippler J and Bohlke T 2012 An algorithm for the generation of silicon nitride structures *J. Eur. Ceram. Soc.* **32** 589–602
[33] Sahu R K and Hiremath S S 2019 *Corona Discharge Micromachining for the Synthesis of Nanoparticles: Characterization and Applications* 1st edn (New York: CRC Press) (https://doi.org/10.1201/9780429275036)
[34] ASM Handbook 1990 *Volume 2: Properties and Selection: Nonferrous Alloys and Special-Purpose Materials* Tenthed (Materials Park, OH: ASM International)
[35] Haizhi Y 2003 An overview of the development of Al-Si alloy based material for engine applications *J. Mater. Eng. Performance* **12** 288–97
[36] Mohanavel V, Rajan K, Kumar S S, Vijayan G and Vijayanand M 2018 Study on mechanical properties of graphite particulates reinforced aluminium matrix composite fabricated by stir casting technique *Mater. Today Proc.* **5** 2945–50
[37] Seah K, Sharma S and Ramesh A 2000 Mechanical properties of cast aluminium alloy 6061-albite particulate composites *Proc of the Institution of Mechanical Engineers, Part L: J. Mater. Design. Applications* **214** 1–6
[38] Ozden S, Ekici R and Nair F 2007 Investigation of impact behaviour of aluminium based SiC particle reinforced metal–matrix composites *Compos. Part A: Appl. Sci. Manuf.* **38** 484–94
[39] Bastwros M, Kim G Y, Zhu C, Zhang K, Wang S, Tang X and Wang X 2014 Effect of ball milling on graphene reinforced Al6061 composite fabricated by semi-solid sintering *Compos. Part* B **60** 111–8
[40] Wang J, Li Z, Fan G, Pan H, Chen Z and Zhang D 2012 Reinforcement with graphene nanosheets in aluminium matrix composites *Scr. Mater.* **66** 594–7
[41] Nayak B, Sahu R K and Karthikeyan P 2018 Study of tensile and compressive behaviour of the in-house synthesized al-alloy nanocomposite *IOP Conference Series: Mater. Sci. Eng.* **402** 1–012070
[42] Rarani M H and Naeini K B K 2018 Micromechanics based damage model for predicting compression behavior of polymer concretes *Mech. Mater.* **117** 126–36